EUROPEAN ORGANIZATION FOR NUCLEAR RESEARCH

CERN/SPSC 99–4
CERN/SPSLC/P264 Add. 3
13. January 1999

ADDENDUM–3 to PROPOSAL SPSLC/P264

# Status and Future Programme of the NA49 Experiment

J. Bächler[5], D. Barna[4], L.S. Barnby[3], J. Bartke[6], R.A. Barton[3], L. Betev[11], H. Bialkowska[14,5], A. Billmeier[10], C.O. Blyth[3], B. Boimska[14], J. Bracinik[19], F.P. Brady[8], R. Brun[5] , P. Buncic[5,10], L.D. Carr[16], G.E. Cooper[2], J.G. Cramer[16], P. Csato[4], V. Eckardt[13], F. Eckhardt[12], T. Empl[20], J. Eschke[7], H.G. Fischer[5], D. Flierl[10], Z. Fodor[4], U. Frankenfeld[7], P. Foka[10,*], P. Freund[13], V. Friese[12], J. Ftacnik[19], J. Gal[4], R. Ganz[13], M. Gaździcki[10], E. Gładysz[6], J. Grebieszkow[15], V. Grogoriev[22], J.W. Harris[17], S. Hegyi[4], V. Hlinka[19], C. Höhne[12], Y. Hu[23], G. Igo[11], M. Ivanov[19], P. Jacobs[2], R. Janik[19], P.G. Jones[3], K. Kadija[18,13], V. Kaplin[22], A.G. Karev[13], V.I. Kolesnikov[9], M. Kowalski[6], B. Lasiuk[17], P. Lévai[4], F. Liu[23], L. Liu[23], V. Loginov[22], U. Lynen[7], A.I. Malakhov[9], S. Margetis[21], C. Markert[7], B. Mayes[20], G.L. Melkumov[9], A. Mischke[12], J. Molnár[4], J.M. Nelson[3], G. Odyniec[2], G. Palla[4], A.D. Panagiotou[1], Y. Pestov[7], A. Petridis[1], M. Pikna[19], L. Pinsky[20], O. Piskunov[22], R.J. Porter[2], A.M. Poskanzer[2], D.J. Prindle[16], F. Pühlhofer[12], J.G. Reid[16], R. Renfordt[10], W. Retyk[15], H.G. Ritter[2], D. Röhrich[10], C. Roland[7], G. Roland[10], A. Rybicki[6], T. Sammer[13], A. Sandoval[7], H. Sann[7], A.Yu. Semenov[9], E. Schäfer[13], R. Schmidt[7], N. Schmitz[13], P. Seyboth[13], F. Sikler[4], B. Sitar[19], E. Skrzypczak[15], M. Spegel[5], G.T.A. Squier[3], H. Stelzer[7], R. Stock[10], P. Strmen[19], H. Ströbele[10], T. Susa[18], I. Szarka[19], I. Szentpetery[4], P. Szymański[5,14], J. Sziklai[4], M. Toy[2,11], T.A. Trainor[16], T. Ullrich[17], M. Vassiliou[1], G. Veres[4], G. Vesztergombi[4], D. Vranic[5,18], F. Wang[2], D.D. Weerasundara[16], S. Wenig[5], C. Whitten[11], N. Xu[2], T.A. Yates[3], I.K. Yoo[12], J. Zimanyi[4], X.-Z. Zhu[16]

[1]Department of Physics, University of Athens, Athens, Greece, [2]Lawrence Berkeley National Laboratory, University of California, Berkeley, USA, [3]Birmingham University, Birmingham, England, [4]KFKI Research Institute for Particle and Nuclear Physics, Budapest, Hungary, [5]CERN, Geneva, Switzerland, [6]Institute of Nuclear Physics, Cracow, Poland, [7]Gesellschaft für Schwerionenforschung (GSI), Darmstadt, Germany, [8]University of California at Davis, Davis, USA, [9]Joint Institute for Nuclear Research, Dubna, Russia, [10]Fachbereich Physik der Universität, Frankfurt, Germany, [11]University of California at Los Angeles, Los Angeles, USA, [12]Fachbereich Physik der Universität, Marburg, Germany, [13]Max-Planck-Institut für Physik, Munich, Germany, [14]Institute for Nuclear Studies, Warsaw, Poland, [15]Institute for Experimental Physics, University of Warsaw, Warsaw, Poland, [16]Nuclear Physics Laboratory, University of Washington, Seattle, WA, USA, [17]Yale University, New Haven, CT, USA, [18]Rudjer Boskovic Institute, Zagreb, Croatia, [19]Comenius University, Bratislava, Slovakia, [20]University of Houston, Houston, TX, USA, [21]Kent State University, Kent, OH, USA, [22]MEPhI, Moscow, Russia, [23]Inst. Part. Phys of Hua Zhong University, Wuhan, China

[*] EC fellow

# 1 Introduction

In January 1998 the NA49 collaboration submitted a detailed report [1] to the SPS committee, presenting the status and future programme of the NA49 experiment.

This report advocated a comprehensive and consistent study of hadronic interactions with the NA49 detector, ranging from the elementary hadron+nucleon processes via hadron+nucleus interactions with controlled centrality, to heavy ion collisions at a variety of nuclear masses and energies.

One of the main motivations for this programme was and is the apparent experimental difficulty to demonstrate the expected transition to a new state of hadronic matter, the Quark Gluon Plasma (QGP), in A+A collisions at the SPS. Although a number of suggestive signatures have been observed in the corresponding hadronic and leptonic final states [2], a convincing and exclusive proof of their origin from QGP formation is still lacking.

This tantalizing situation has its origin both in the insufficient experimental exploration of the soft hadronic sector in general, and in the evident theoretical difficulties in handling non-perturbative phenomena in the framework of QCD [3].

The NA49 experimental programme is expected to lead to a significant improvement of understanding of strong interactions. In particular, the hypothesis of QGP production can be confirmed (or falsified) by searching for the phase transition region at low collision energy and low masses of colliding nuclei. The relevant observables used in this search are pion and strangeness yields, properties of the expansion of the system measured by the hadronic spectra and two particle correlations, and event-by-event fluctuations.

During the past year the NA49 collaboration has vigorously pursued its experimental programme. New data with Pb ions at reduced energy (a modest test sample so far) and with secondary ion beams have been obtained. New detector components have been added to the existing detector layout in connection with developments for the ALICE detector. Progress in data analysis and interpretation, notably concerning particle identification, now allows a detailed comparison of data sets over the full range of hadronic interactions available at the SPS [4].

The present addendum contains in section 2 a report on the ongoing experimental developments. Section 3 offers examples of ongoing physics analysis, with emphasis on the unique coverage of different hadronic interactions by the NA49 detector. An update of the NA49 beam requests for the years 1999 and 2000 is presented in section 4. Section 5 outlines plans for a physics programme beyond the year 2000.

# 2 Experimental Developments

## 2.1 Secondary Ion Beams

The final states of central collisions of heavy nuclei and nucleon+nucleon interactions differ substantially. It is therefore crucial for an understanding of the origin of the observed differences to study their development with increasing size of the colliding nuclei. Therefore we have chosen to devote part of our 1998 Pb run time to an experimental investigation of $^{12}$C+$^{12}$C and $^{28}$Si+$^{28}$Si collisions.

This programme was made possible through the generation of a secondary fragmentation beam which was produced by a primary target (1 cm carbon) in the extracted Pb–beam approximately 30 m downstream of the H2/H4 splitter. With the beam line momentum set to 316 GeV/c a large fraction of all $Z/A = 1/2$ fragments was transported to the NA49 experiment. Online selection based on a pulse height measurement in a scintillator beam counter was used to select particles with $Z = 6$ (Carbon) and $Z = 13$, 14, 15 (Al, Si, P). Offline cleanup is achieved by using in addition the energy loss measured in 6 MWPCs which also measure the beam position (BPDs). The resolution of the combined pulse height measurement can be deduced from the pulse height spectrum shown in Fig. 1. A clear $Z$-separation is achieved all the way from Boron to Phosphorous.

During a period of 14 days 500 k C+C and 400 k (Al,Si,P)+Si events were recorded. A first look at the multiplicity of the produced charged particles (vertex tracks) as function of the forward going energy Eveto in spectator fragments is given in Fig. 2. One finds that in the most central collisions in C+C (Si+Si) the averaged multiplicity of accepted charged particles reaches 70 (150) as compared to about 900 in central Pb+Pb collisions at 158 A·GeV.

## 2.2 40 A·GeV Central Pb+Pb Collisions

At the end of the 1998 Pb–beam physics period the extraction of 40 A·GeV Pb-ions was set up in an SPS machine development run. The H2 beam line received beam for about 24 hours, during which NA49 recorded about 30k central Pb+Pb collisions. In order to keep the acceptance of the detector similar to the full energy runs, the magnetic field in the Vertex Magnets was reduced to 1/4. A preliminary plot of the uncorrected charged particle event multiplicity (vertex tracks) versus the energy of the spectator beam nucleons is shown in Fig. 3.

## 2.3 Forward TPC

During the 1998 heavy ion run a new small Time Projection Chamber, the forward TPC was added to the tracking detectors of NA49 [1]. This TPC serves the double purpose of testing new detector and electronics concepts for the proposed ALICE TPC in a realistic high track–density environment, and to improve the forward acceptance of NA49 in the region of $x_F \geq 0.6$. This new TPC as well as the corresponding new front–end and digitization electronics have been successfully operated and integrated, via a newly developed Digital Data Link, into the NA49 data acquisition system.

## 2.4 PesTOF Detector

A set of seven PesTOF detectors was for the first time tested in the high multiplicity environment of central Pb+Pb collisions. 40 k events were recorded at detector voltages of

4.5 kV and at 4.75 kV, respectively and about 3 k events at 5.0 kV. In addition for about 20 k events the main gas mixture component Argon was replaced by Neon. A sizable fraction of the events had more than one hit per counter. The acquired statistics should be sufficient to determine the time and position resolution as a function of occupancy, HV, and gas composition. Fig. 4 shows the 2–dimensional position distribution of hits in the counter array for a selected event.

### 2.5 Status of Computer Facilities

Over the past five years the NA49 collaboration, faced with data volumes of tens of terabytes each year, has developed and deployed original data handling packages like DSPACK [5] and ROOT [6] which have subsequently been adopted and used by the wider HEP community. In order to keep up with 50 TByte of raw and reconstructed data gathered so far, the migration from an expensive workstation based computing environment to a relatively cheap and cost effective PC architecture was accomplished in 1998. This corresponds to an increase by a factor of 6 in CPU power dedicated to reconstruction and analysis, thus preparing the ground for important new data volumes to be gathered over the coming years.

## 3 Examples of Ongoing Physics Analysis

During last year the NA49 Collaboration obtained final results on several subjects in hadron production in Pb+Pb collisions at 158 A·GeV, namely:

- spectra and yields of baryons [7],
- spectra and yields of negatively charged hadrons [7],
- data on directed and elliptic flow of protons and charged pions [8],
- data on transverse momentum event–by–event fluctuations [9],
- spectra and yields of $\Xi^-$ and $\overline{\Xi}^+$ hyperons [10],
- data on the composition of projectile spectator matter [11].

In parallell, significant progress has been made in the analysis of p+p and p+Pb events recorded by the NA49 detector. The addition of a centrality detector [1] to the NA49 detector allows the high statistics study of hadron+nucleus collisions with controlled participant number as one of the important links between hadron+nucleon and nucleus+nucleus processes. Preliminary data on p+p and p+Pb collisions will be discussed along with the Pb+Pb results.

### 3.1 Longitudinal Momentum Spectra

Longitudinal momentum distributions for baryons and mesons carry important information about baryon number transfer (”stopping”) and the build-up of energy density as well as expansion dynamics and yields of produced particles.

The rapidity distribution of baryons participating in central Pb+Pb collisions, plotted in Fig. 5, is similar to the distribution for central S+S collisions [7]. However both distributions are much more centered at midrapidity than the corresponding, strongly forward-backward peaked distribution for p+p interactions at the same collision energy per nucleon. These results seem to indicate that the conditions during the early stage of the collisions (energy and baryon density) are similar for central S+S and Pb+Pb collisions but they are different for p+p interactions.

The rapidity distributions of negatively charged hadrons (about 85% $\pi^-$–mesons) for central S+S and Pb+Pb collisions (see Fig. 6) are similar in shape, but the yield per participant nucleon at midrapidity is about 40% larger in nucleus+nucleus collisions than the corresponding yield for p+p interactions [7], while the overall increase of pions per participant nucleon is of

about 25% (going from p+p to Pb+Pb). This confirms earlier observation of a pion enhancement effect in central A+A collisions at the SPS, which should be confronted with pion suppression observed at AGS and lower energies [12]. We note that enhanced production of pions is expected in case of Quark Gluon Plasma creation due to increased entropy production. The observation of an onset of the pion enhancement when going from low to high collision energies is a possible indicator of the beginning of the phase transition region [12].

A complementary view of these spectra is given by the $x_F$-distributions of participating protons (p–$\overline{\mathrm{p}}$) and of the mean of charged pions (($\pi^+ + \pi^-$)/2). In Fig. 7 they are compared for p+p, peripheral and central p+Pb, as well as central Pb+Pb collisions. A change of the baryonic and mesonic spectra is apparent in these widely different hadronic interactions. The pion yield in central Pb+Pb interactions, scaled with the assumption of 176 participant nucleon pairs [7], shows a remarkable similarity with p+p and peripheral p+A collisions over about 2 orders of magnitude in cross section except in the central region around $x_F = 0$, where the p+p point lies below (see Fig. 7a). A steepening of the $x_F$-distribution is however observed in central p+Pb collisions. A more marked dependence on reaction type is observed in the p–$\overline{\mathrm{p}}$ yields (Fig. 7b), where the scaled $x_F$-distribution for Pb+Pb falls well below the p+p and peripheral p+Pb curves. Note that the central p+Pb curve turns out to be even below the central Pb+Pb result. Here, isospin effects in the proton yield from neutron projectiles as observed in Pb+Pb have to be further investigated. The interpretation of this complex phenomenology can make full use of our handles on projectile type, system size, impact parameter and beam energy.

### 3.2 Transverse Momentum Behaviour

The study of transverse momentum phenomena and their dependence on particle and reaction type can be carried out in NA49 over a large fraction of the available phase space. As an example of the ongoing detailed analysis, Fig. 8 shows the mean transverse momentum (i.e. the first moment of the corresponding distribution) for pions and protons as function of $x_F$ for p+p, p+Pb and Pb+Pb interactions. As in the case of the longitudinal variables, a dependence of the transverse momentum distribution on the reaction type is evident. For pions, the well-known "seagull" structure in p+p reactions steepens up with increasing centrality in p+Pb collisions whereas central Pb+Pb events show an intermediate behaviour close to peripheral p+Pb interactions. The detailed role of resonance decays in this phenomenon remains to be elucidated. For protons, on the other hand, the $x_F$–dependence is rather flat throughout, with a clear increase of the mean $p_T$ up to central Pb+Pb interactions. Studies of this type, including of course also higher moments characteristic of the shape of the distributions, should shed some light on the underlying production mechanisms like transverse expansion or multiple projectile scattering.

Another important global variable accessible to NA49 is the event-by-event fluctuation of transverse momentum shown in Fig. 9 for central Pb+Pb collisions [9]. The fluctuation turns out to be compatible with independent particle production. This is in line with the fluctuations expected from thermal equilibrium models [13]. The high statistics and high resolution of these data allow NA49 to set an upper limit on the production of Disoriented Chiral Condensates in central Pb+Pb collisions at the SPS.

### 3.3 Strangeness Production

Strangeness production and its increase in central heavy ion collisions have received much attention, especially in view of possible interpretations in the framework of QGP formation. The analysis of strange and nonstrange hadron production in high energy interactions

($e^+$+$e^-$, p+p, p+$\overline{p}$, p+A, and A+A collisions) shows an enhancement of the total (integrated over all of phase space) production of $s$ and $\overline{s}$ quarks in central nucleus+nucleus collisions (see Fig. 10, [16, 17]). This enhancement can be described by a model assuming the creation of a globally equilibrated Quark Gluon Plasma in the early stage of the collision [18].

The distribution of strangeness over momentum space and over different species of hadrons shows however a complicated pattern. The detailed investigation of this pattern is possible in NA49, largely due to recent improvements in particle identification by $dE/dx$ methods covering most of the acceptance available for tracking. In Fig. 11 the invariant cross sections of charged kaons and pions are shown as function of $x_F$ for the reactions p+p, central p+Pb, and central Pb+Pb. The known overall increase of these ratios going from p+p to Pb+Pb collisions is clearly evident in the more detailed dependences on the kinematical variables. However, also p+Pb collisions reveal an increase of roughly the same size and systematics, observable over the complete projectile hemisphere. This is clearly seen in Fig. 11 for central p+Pb collisions ($p_T$–range 400–500 MeV/c).

Fig. 12 shows the K/$\pi$ ratios as function of centrality of p+Pb collisions ($N_{CD}$) for three $p_T$–ranges (at $x_f = 0.05$). For comparison, the ratios for p+p and Pb+Pb collisions are plotted at $N_{CD} = 0$ and $N_{CD} = 11$, respectively. Apart from the (trivial) fact that the K/$\pi$ ratios increase with $p_T$ for all reactions due to the larger mean $p_T$ of kaons, a general relative increase of comparable size from p+p via p+Pb to Pb+Pb is seen at all $p_T$. A more detailed analysis of this transition, including the question whether there is a saturation effect of this increase at large centrality in p+Pb collisions, requires larger event samples than currently available.

A similar phenomenon is observed for the $\Lambda$–yields. Fig. 13 shows $\Lambda$/$h^-$ ratios referred to the same ratios in p+p, for three different bins of centrality in p+Pb. One should note that unlike Pb+Pb the p+Pb collision system is not symmetric around midrapidity and the NA49 results cannot be extrapolated to full phase space. In fact an increase in the strange particle to pion ratio in the projectile hemisphere appears to be compensated by a decrease in the target hemisphere. Based on the new detailed p+Pb results one can hope to be able to make a better prediction of a purely hadronic scenario for Pb+Pb interactions.

It is obviously interesting and necessary to perform the same analysis for other strange particles, e.g. the $\Xi^-$ which has recently been shown to exhibit a large enhancement factor of about 10 in central Pb+Pb events [10] compared to p+p reactions. The $\Xi^-$–yield measured in NA49 for central Pb+Pb collisions is presented in Fig. 14. Precise reference data in p+p and central p+Pb collisions in NA49 are required and would greatly benefit from increased statistics in both cases.

### 3.4 Spectroscopy: The Example of Phi Production

Up to now, spectroscopy in central Pb+Pb interactions is limited – due to overwhelming combinatorial background – to rare leptonic decay modes or to narrow resonances like $\Lambda(1520)$ or $\Phi$. The $\Phi$-meson study in NA49 indeed offers the possibility to follow the detailed evolution of the differential cross section through the different hadronic interactions. Fig. 15 and Fig. 16 show $y$– and $p_T$–distributions of the $\Phi$ obtained in p+p and central Pb+Pb events respectively. Both distributions reveal a broadening when going from p+p collisions to central Pb+Pb interactions. The $\Phi$–production cross section with respect to the $\pi$–production increases by a factor of 2.1. A total inclusive cross section of 470 $\mu$barn has been determined in p+p collisions. In p+Pb collisions the yield is again a function of centrality. Fig. 17 shows $\Phi$/$h^-$ ratios for $y \geq 2.5$, referred to p+p, for three centrality bins. A clear increase of this ratio is observed towards the value for central Pb+Pb.

### 3.5 Bose-Einstein Correlations

The detailed study of Bose-Einstein correlations of identical particle pairs has been one of the main experimental objectives of NA49 from its conception. These results together with the data on longitudinal and transverse momentum single particle spectra have been used to extract information on the space–time structure of the collision region in central Pb+Pb collisions [14]. The BE-correlation study is now extended for the first time to correlations in all three components of the relative momentum $Q$ also in p+p and p+Pb interactions. Due to limited event statistics only four bins of phase space could be used: average transverse momentum $k_T \leq 0.2$ and $0.2 \leq k_T \leq 0.8$ GeV/c, pair rapidity $1.9 \leq y \leq 3.9$ and $3.9 \leq y \leq 5.8$.

The correlation functions for p+p and central Pb+Pb collisions are compared in Fig. 18 for central rapidity. The expected narrowing of the correlation structure with increasing system size is clearly visible. Corresponding radius parameters have been extracted from 3–dimensional fits using the Bertsch–Pratt parametrization. They are given in Fig. 19 as function of $k_T$ for p+p, p+Pb at different centralities, and central Pb+Pb. For ease of comparison, the radii observed for Pb+Pb collisions have been scaled down by the geometry factor $\mathrm{A}^{-1/3} = 1/6$. The transverse radii are in reasonable agreement with this scaling in particular when comparing p+p to Pb+Pb results. Significant deviations show up in longitudinal direction. It is surprising that the $k_T$–dependence of the transverse radii is similar since the importance of transverse collective expansion and of the resonance decay halo are expected to be rather different in Pb+Pb and p+p reactions.

It should be mentioned that more detailed studies for p+p and p+Pb will become possible with the availability of data samples with substantially increased statistics.

### 3.6 Peripheral Pb+Pb Reactions and Study of Flow Phenomena

The trigger system of NA49 has recently been upgraded with a He–Cerenkov counter offering high resolution on projectile charge [4]. Placed in anti-coincidence immediately downstream of the Pb–target, it allows for effective triggering on peripheral Pb+Pb events with low background. A large data sample with impact parameters up to about 10 fm has thus been obtained.

In these non-central collisions the interaction (overlap) region is a lens–shaped object. Transverse flow of produced particles may then reflect this anisotropy in an azimuthally nonuniform momentum or particle number distribution. Elliptic flow is quantified by the coefficient of the second harmonic in the Fourier expansion of the transverse azimuthal distribution of particles relative to the reaction plane which is determined event–by–event. The strength of the flow is one of the few hadronic signals related to the equation of state of matter at high density. Fig. 20 shows the elliptic flow of pions as function of rapidity for impact parameters between 6 and 8 fm. Comparison with string–hadronic models [15] indicates more flow at mid–rapidity and hence a harder equation of state than assumed in these models.

## 4 Update of Beam Requests in 1999 and 2000

### 4.1 Pb Beam in 1999

The NA49 collaboration has requested 28 days of Pb–beam at 40 GeV/c per nucleon and 14 days at 80 GeV/c per nucleon during the heavy ion run in 1999 [1]. This request is based on the following considerations:

– Results on Pb+Pb collisions at 40, 80 and 158 GeV/c per nucleon will constitute a rich and consistent set of data obtained by a single experiment which, together with the currently measured energy dependence at the AGS [19] should substantially improve our understanding of the properties of strongly interacting matter at high energy density.
– Should the present experimental signatures indeed correspond to QGP formation at the top SPS energy this would imply a phase transition located at lower energies. Calculations concerning the location of this transition region are model dependent. It can however be estimated that the minimum width in energy of the transition region should be in the range 30–40 GeV/c per nucleon. Therefore results at more than one reaction energy are crucial for any attempt at localization of this transition.
– Different experimental signatures of the phase transition may reach their maximum significance at different points of the transition region. Therefore results at 40 and 80 GeV/c per nucleon could allow to observe more than one signature.

A unique feature of the large acceptance of the NA49 experiment is the possibility to study most of the relevant observables with moderately large event samples of few times $10^5$ central nucleus+nucleus collisions. Therefore the beam time needed to obtain a significant sample can be relatively short, of the order of one week. This is not necessarily the case for the other heavy ion experiments. In case of a collision of interest, the requested Pb–beam time at 80 GeV/c per nucleon could therefore be reduced to one week.

### 4.2 Pb beam in 2000

In order to study system size dependence, S– and Ag–beams at 158 GeV/c per nucleon were requested in the previous addendum [1]. Due to the successful production of secondary C– and Si–beams already this year, the request for S–beam in 2000 can be replaced by Ag–beam for the whole running period.

### 4.3 Proton beam

Our present data samples in p+p and hadron+Pb interactions correspond to about $4 \cdot 10^5$ events each after cuts, obtained in about 4 weeks of beam time both in 1996 and 1997.

In 1998, the planned data taking period in August/September was lost due to a serious problem with one of the superconducting Vertex Magnets.

At present, 4 1/2 weeks of running with hadron beams are foreseen for the fall period in 1999. We request a similar period of beam time for the year 2000.

## 5 Physics Programme Beyond 2000

As explained above, the NA49 collaboration is at present entering into a phase of opening up its experimental programme both in the heavy ion sector and concerning the more elementary hadron+proton and hadron+nucleus interactions. Data reduction of the resulting large and diverse data samples does not present any technical problems due to the impressive progress in parallel computing using PC farms at CERN. Physics analysis is following up these new directions with the hope to decisively improve the understanding of hadronic phenomena in general and of the hypothetical transition to QGP formation in particular. The collaboration is looking forward to two more data taking periods in the framework of the approved heavy ion programme at the SPS.

There are however a few points which already now merit contemplation of a possible extension of the physics programme beyond the year 2000. These points concern running with ion beams and with hadron beams. They should be seen also in the context of the complementarity of the NA49 programme with other fixed target activities beyond 2000 at CERN.

### 5.1 Hadron+Nucleon Physics

Keeping in mind that NA49 is the only large solid angle detector facility with wide particle identification coverage still active in the SPS energy range, and regarding the physics possibilities opening up after the first round of data taking and analysis, further running periods beyond 2000 seem certainly worth considering. Data samples of several million events with proton and pion beams would allow a decisive step forward not only in reference to heavy ion phenomena but also in the more detailed understanding of soft hadronic physics in connection with non-perturbative QCD.

### 5.2 Hadron+Nucleus Physics

The first running period using nuclear targets with centrality selection in 1997 was used to explore the possibilities of NA49 in this field in a variety of conditions. Data with proton and pion beams on Al– and Pb–targets were obtained at two beam energies. These event samples of typically $10^4$–$10^5$ events are being studied in view of isolating those physics items which merit more detailed inspection. There is no doubt that also in this field a further substantial increase of event statistics will allow new and deeper insight into many problems connected with propagation and interaction of hadronic probes in nuclear matter.

### 5.3 Further Studies with Nuclear Beams

With the opening of parameter space in nuclear interactions concerning system size and interaction energy further insight into the hypothesis of phase transition to QGP is expected. The obvious further goal of NA49 would be the more detailed study of this phenomenon. The request for extended ion beam operation will depend on the results of the data taken in 1999 and 2000.

### 5.4 Study of Open Charm Production in Heavy Ion Collisions

The extension of the detection capabilities of NA49 to the lowest lying heavy flavour states would constitute an obvious physics interest. Charm production mechanism and cross section in nuclear matter, especially in high energy density environments, are at present subject to very different model approaches ranging from perturbative QCD to a phenomenological statistical description. The complicated phenomenology of $J/\psi$ production and suppression is intimately connected to open charm processes. The intermediate mass dilepton spectrum measured in Pb+Pb collisions at the SPS [20] shows a strong deviation from perturbative calculations which could be connected with enhanced charm production.

Due to its low production cross section and short life time the measurement of D–meson production in the high multiplicity environment of nucleus+nucleus collisions constitutes a challenging experimental adventure. In collaboration with INFN Torino (L. Riccati, P. Giubellino, F. Tosello, P. Cerello) the NA49 collaboration is presently investigating the feasibility of a vertex detector upgrade of the NA49 detector. Open charm would be studied using

the hadronic decays of $D^0 \rightarrow K^-\pi^+$ and $D^+ \rightarrow K^-\pi^+\pi^+$ (and their respective antiparticles). The D decay vertices are identified using a silicon vertex detector with the addition of particle identification and tracking information from the NA49 detector. The strength of this combination comes from $dE/dx$ identification over a large range in momentum and from the excellent momentum resolution of the NA49 spectrometer, which are vital characteristics in optimizing the signal/background ratio of this measurement. The feasibility of a second level trigger based on on-line tracking from Si–pixel layers in the vertex detector is also studied in order to enhance the data sample within the limitations of beam rate of the NA49 detector to up to $10^8$ central A+A collisions.

The time scale of this charm upgrade of the NA49 experiment would require the availability of ion beams also after the year 2000.

**References**


[1] J. Bächler et al. (NA49 Collab.), *Status and Future Programme of the NA49 Experiment, Addendum–2 to Proposal SPSLC/P264*, CERN/SPSC 98–4, January 1998.

[2] for recent review see: U. Heinz, (Quark Matter 97), Nucl Phys. **A638** (1998) 357c and J. P. Blaizot, (Quark Matter 97), Nucl Phys. **A638** (1998) 373c.

[3] for recent review see: Yu. L. Dokshitzer, (Quark Matter 97), Nucl Phys. **A638** (1998) 291c and hep–ph/9812252.

[4] S. Afanasiev et al. (NA49 Collab.), *The NA49 Large Acceptance Hadron Detector*, CERN–EP/99–001.

[5] P. Buncic and R. Zybert, *DSPACK: Object Manager for High Energy Physics*, Proceedings of International Conference on Computing in High Energy Physics, CHEP'95 Rio de Janeiro, Brazil, World Sci. Singapore (1996) 345.

[6] R. Brun and F. Rademakers, *ROOT: An Object Oriented Data Analysis Framework*, Proceedings of AIHENP'96 Workshop, Lausanne, 1996; Nucl. Instr. and Meth. **A389** (1997) 81.

[7] H. Appelshäuser et al. (NA49 Collab.), nucl–ex/9810014, submitted to Phys. Rev. Lett.

[8] H. Appelshäuser et al. (NA49 Collab.), Phys. Rev. Lett. **80** (1998) 4136.

[9] H. Appelshäuser et al. (NA49 Collab.), IKF–HENPG/1–99.

[10] H. Appelshäuser et al. (NA49 Collab.), Phys. Lett. **B444** (1998) 523.

[11] H. Appelshäuser et al. (NA49 Collab.), Eur. Phys. J. **A2** (1998) 383.

[12] M. Gaździcki and D. Röhrich, Z. Phys. **C65** (1995) 215 and Z. Phys. **C71** (1996) 55.

[13] St. Mrówczyński, Phys. Lett. **B439** (1998) 6.

[14] S. Chapman, P. Scotto and U. Heinz, Heavy Ion Physics **1** (1995) 1 and H. Appelshäuser et al. (NA49 Collab.), Eur. Phys. J. **C2** (1998) 661.

[15] H. Sorge, Phys. Rev. Lett. **78** (1997) 2309 and K. Werner, Phys. Lett. **B208** (1988) 520.

[16] H. Białkowska et al., Z. Phys. **C55** (1992) 347.

[17] F. Becattini, M. Gaździcki, J. Sollfrank, Eur. Phys. J. **C5** (1998) 143.

[18] M. Gaździcki, J. Phys. **G23** (1997) 1881; M. Gaździcki and M. I. Gorenstein, hep–ph/9803462.

[19] R. Ganz et al. (E917 Collab.), 4th International Conference on Strangeness in Quark Matter, Padova, Italy, 20–24 Jul 1998, nucl–ex/9808007.

[20] E. Scomparin et al. (NA50 Collab.), *Strangeness in Quark Matter 98 Conference*, Padova, July 20-24, 1998.

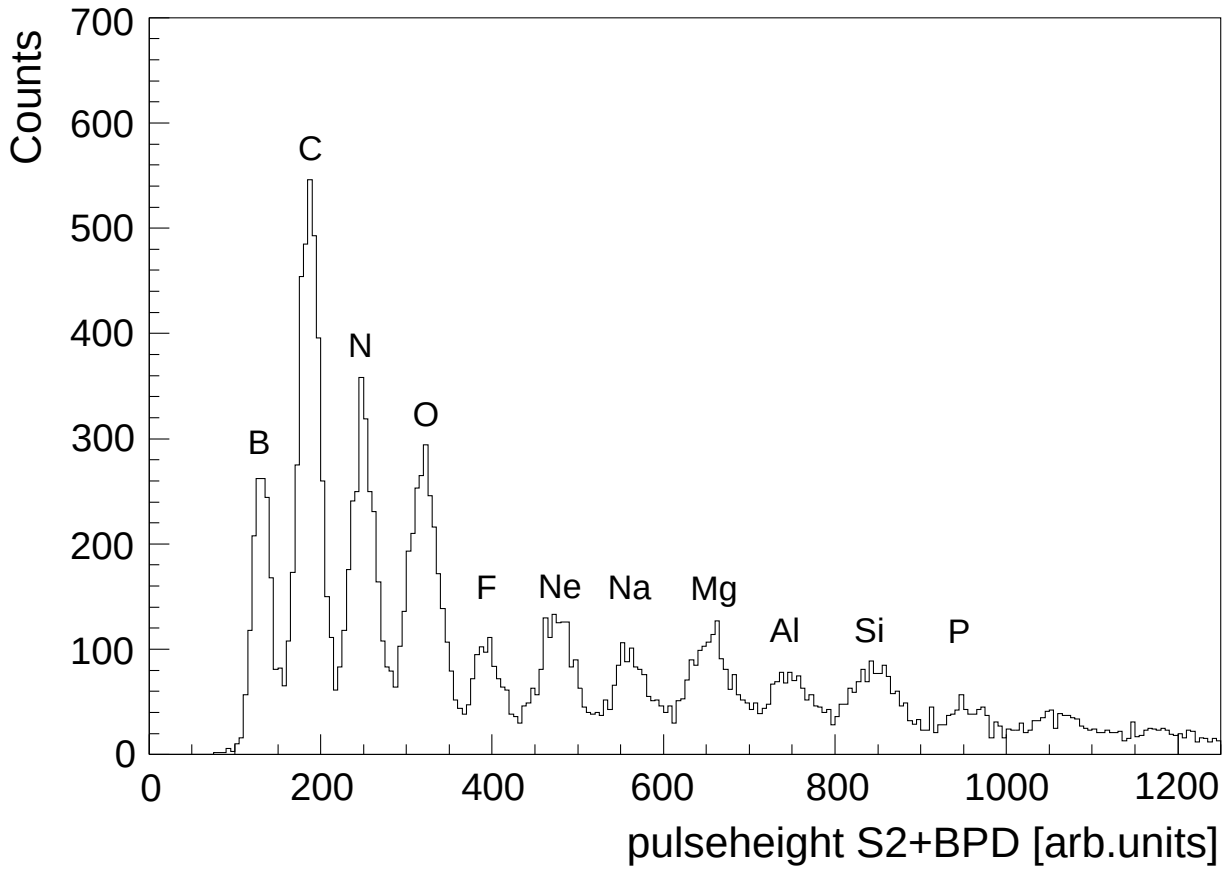


Figure 1: Pb-beam fragmentation spectrum from a 10 mm Carbon target with the beam line set to select $Z/A = 1/2$.

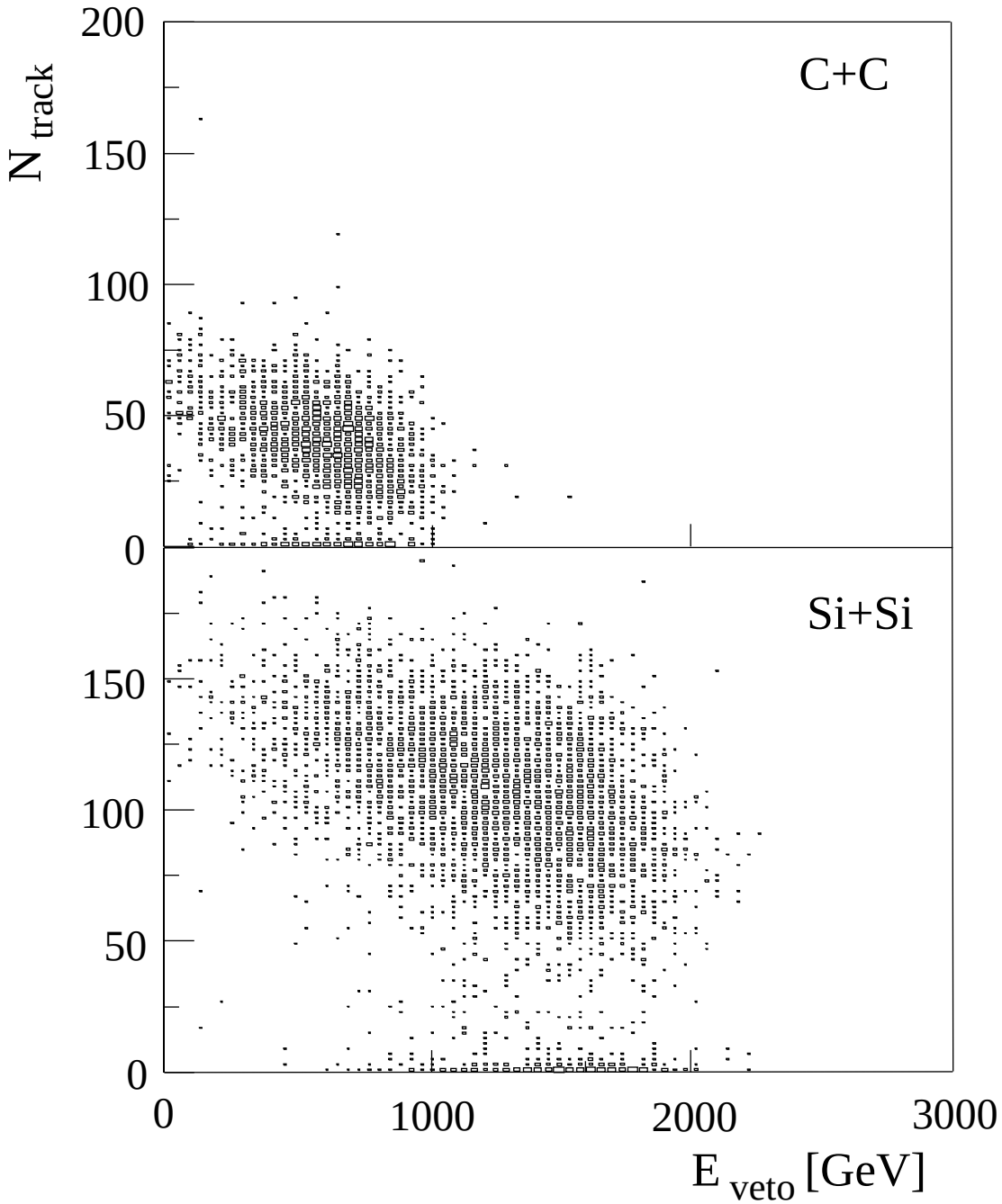


Figure 2: Uncorrected charged particle multiplicity (accepted vertex tracks) as a function of forward going energy measured by the Veto Calorimeter of NA49 for samples of C+C and Si+Si collisions at 158 A·GeV taken during the 1998 Pb–ion run.

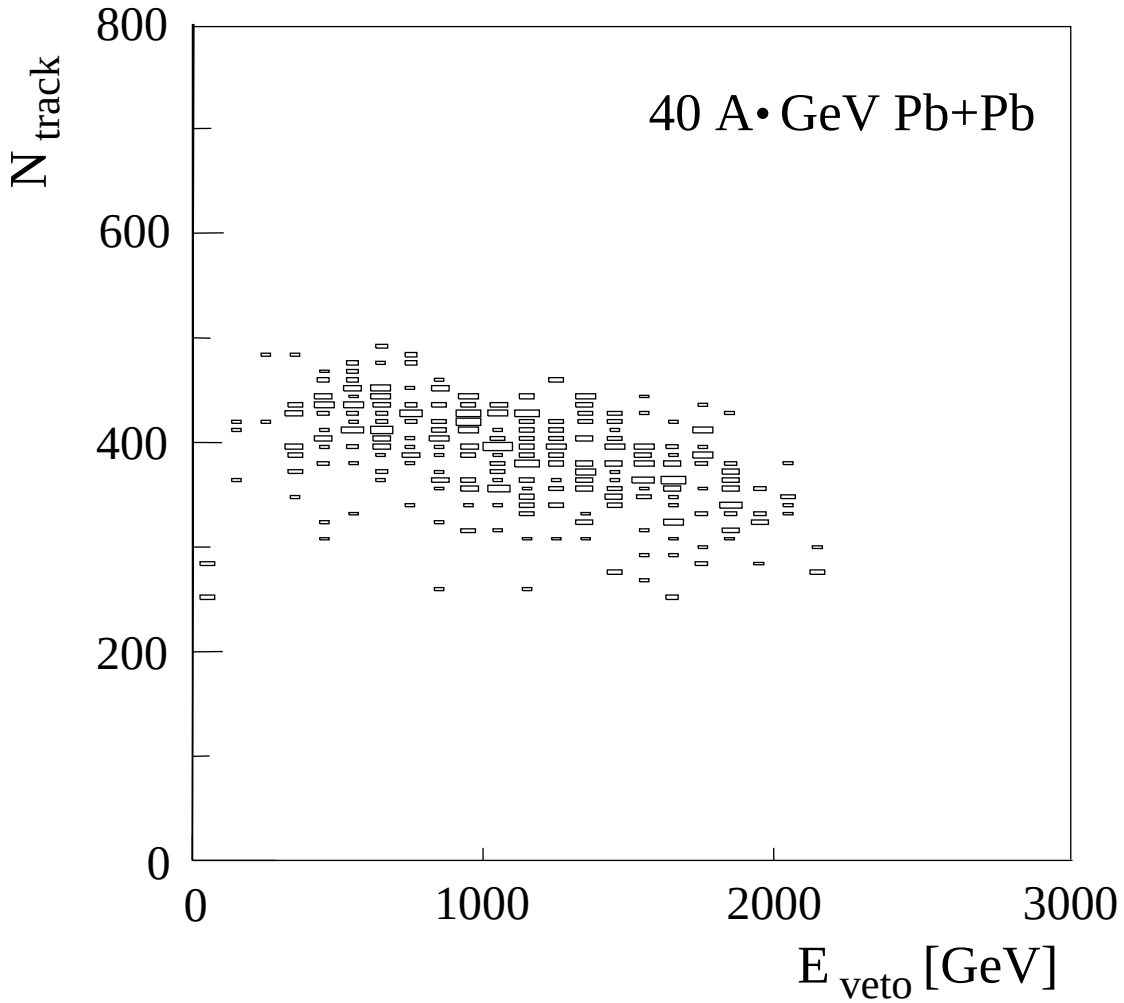


Figure 3: Uncorrected charged particle multiplicity (accepted vertex tracks) as a function of forward going energy measured by the Veto Calorimeter of NA49 for central Pb+Pb collisions at 40 A·GeV taken during the 1998 Pb–ion run.

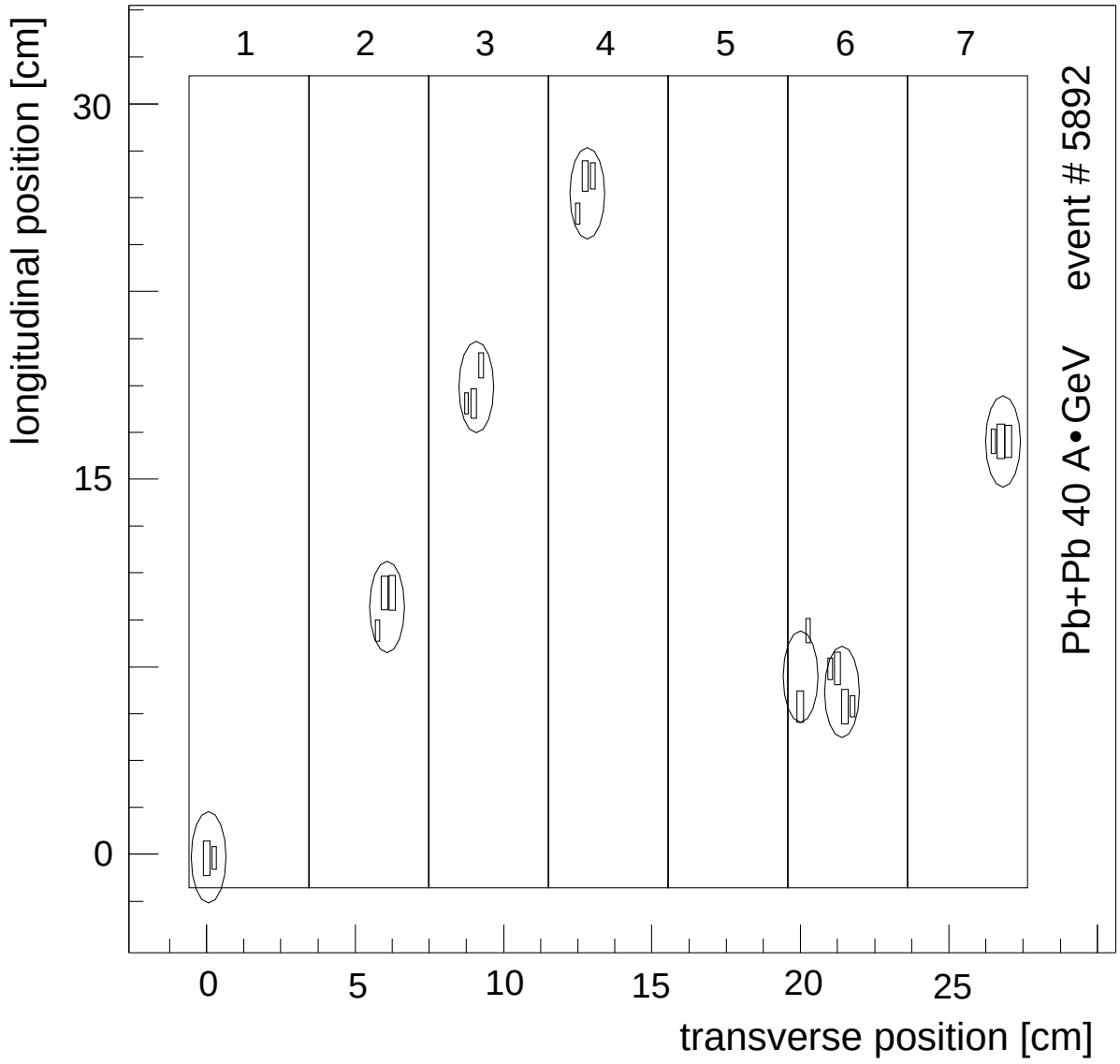


Figure 4: 2-dimensional position distribution of hits in the PesTOF counter array for a selected event.

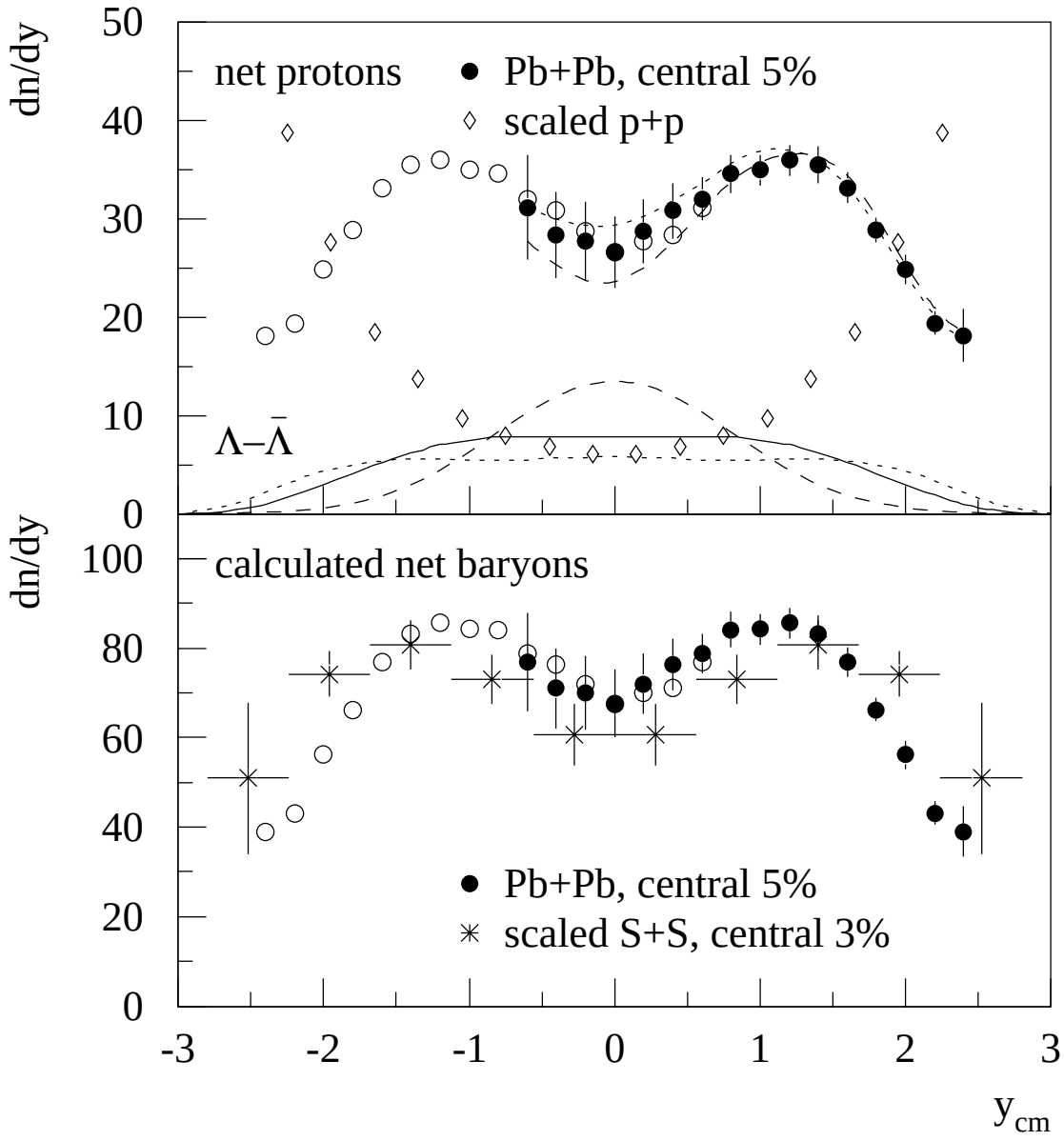


Figure 5: Rapidity distributions of net protons and net baryons produced in central Pb+Pb collisions at 158 GeV/c per nucleon compared to the corresponding distributions for p+p and central S+S collisions scaled by the ratio of number of participant nucleons. (Open circles are data points reflected around $y_{cm} = 0$.)

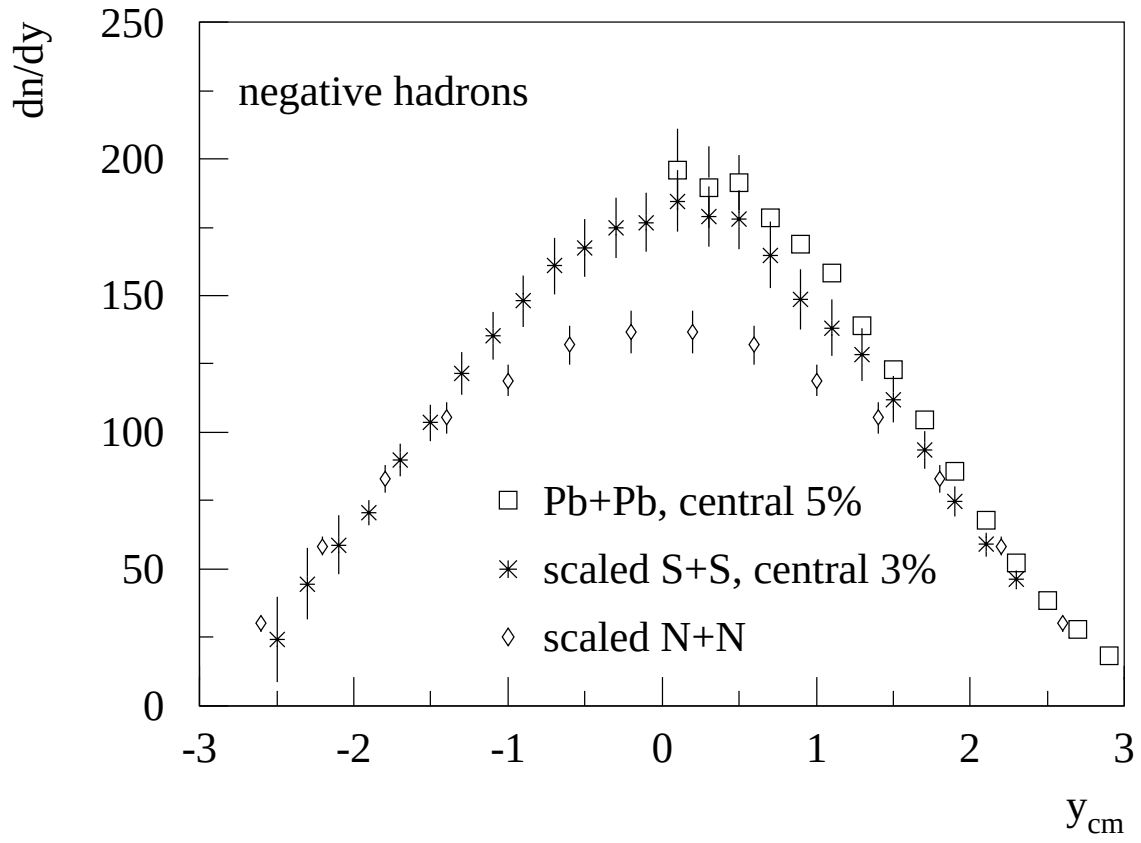


Figure 6: Rapidity distribution of negatively charged hadrons produced in central Pb+Pb collisions at 158 GeV/c per nucleon compared to the corresponding distributions for nucleon+nucleon and central S+S collisions scaled by the ratio of number of participant nucleons [7].

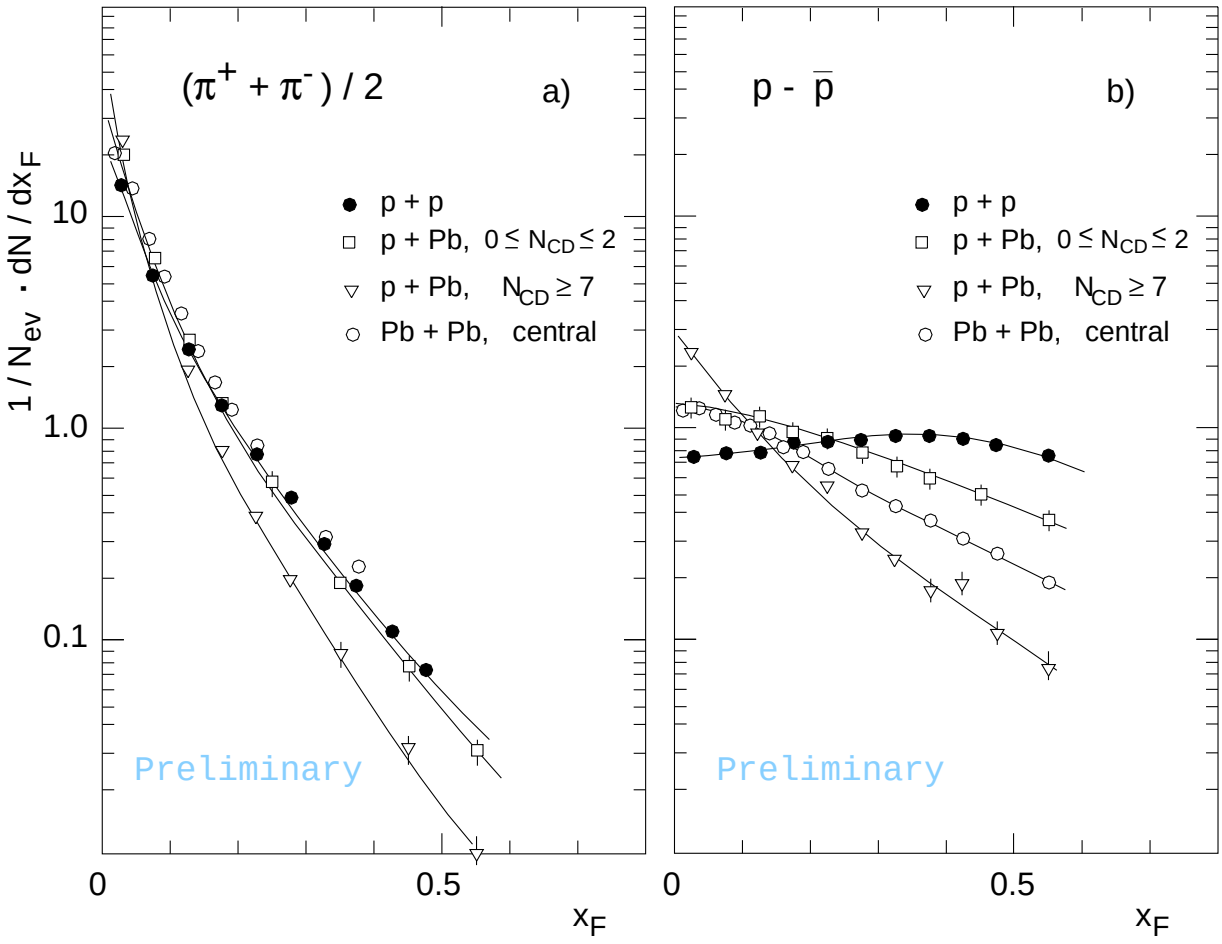


Figure 7: $x_F$ distributions for a) mean charged pions and b) participating protons observed in p+p, peripheral and central p+Pb, as well as central Pb+Pb collisions. The central Pb+Pb results are scaled down by 176 (assumed number of participant nucleon pairs [7]).

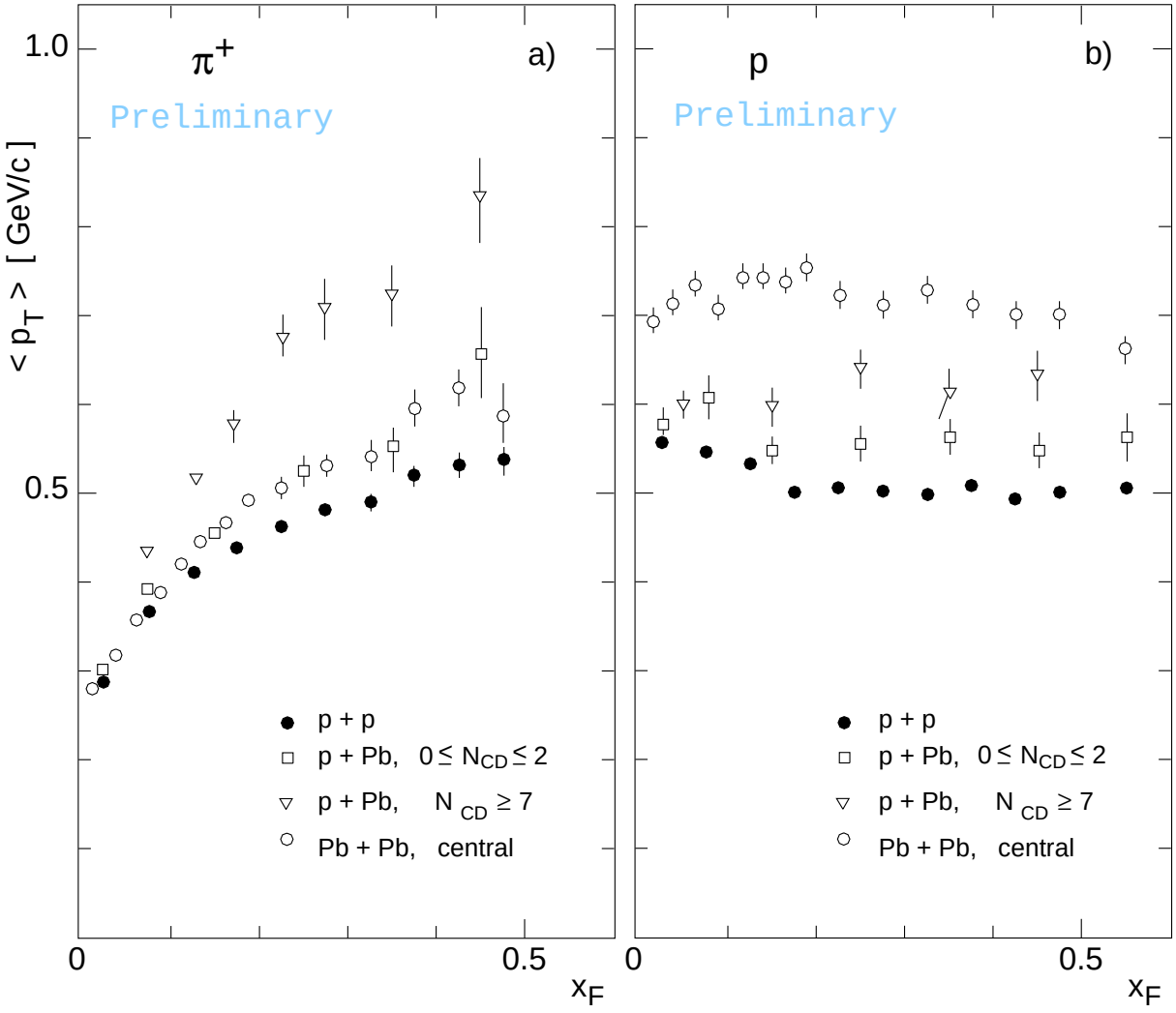


Figure 8: Mean $p_T$ as function of $x_F$ for a) positive pions and b) protons observed in p+p, peripheral and central p+Pb, as well as central Pb+Pb collisions.

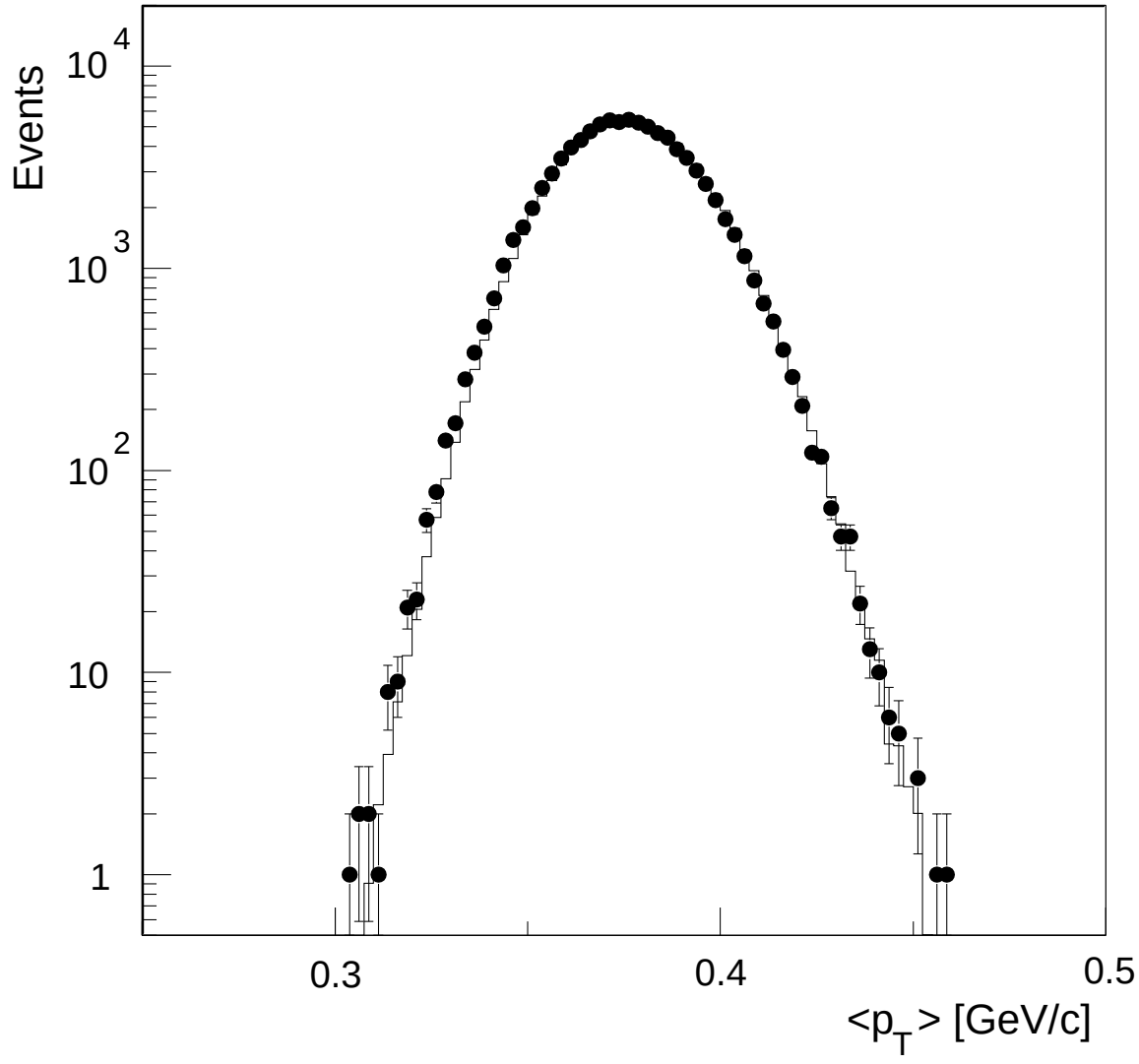


Figure 9: Event–by–event fluctuations of average transverse momentum of charged particles produced in central Pb+Pb collisions at 158 GeV/c per nucleon (points) compared to the distribution obtained assuming independent particle production (line).

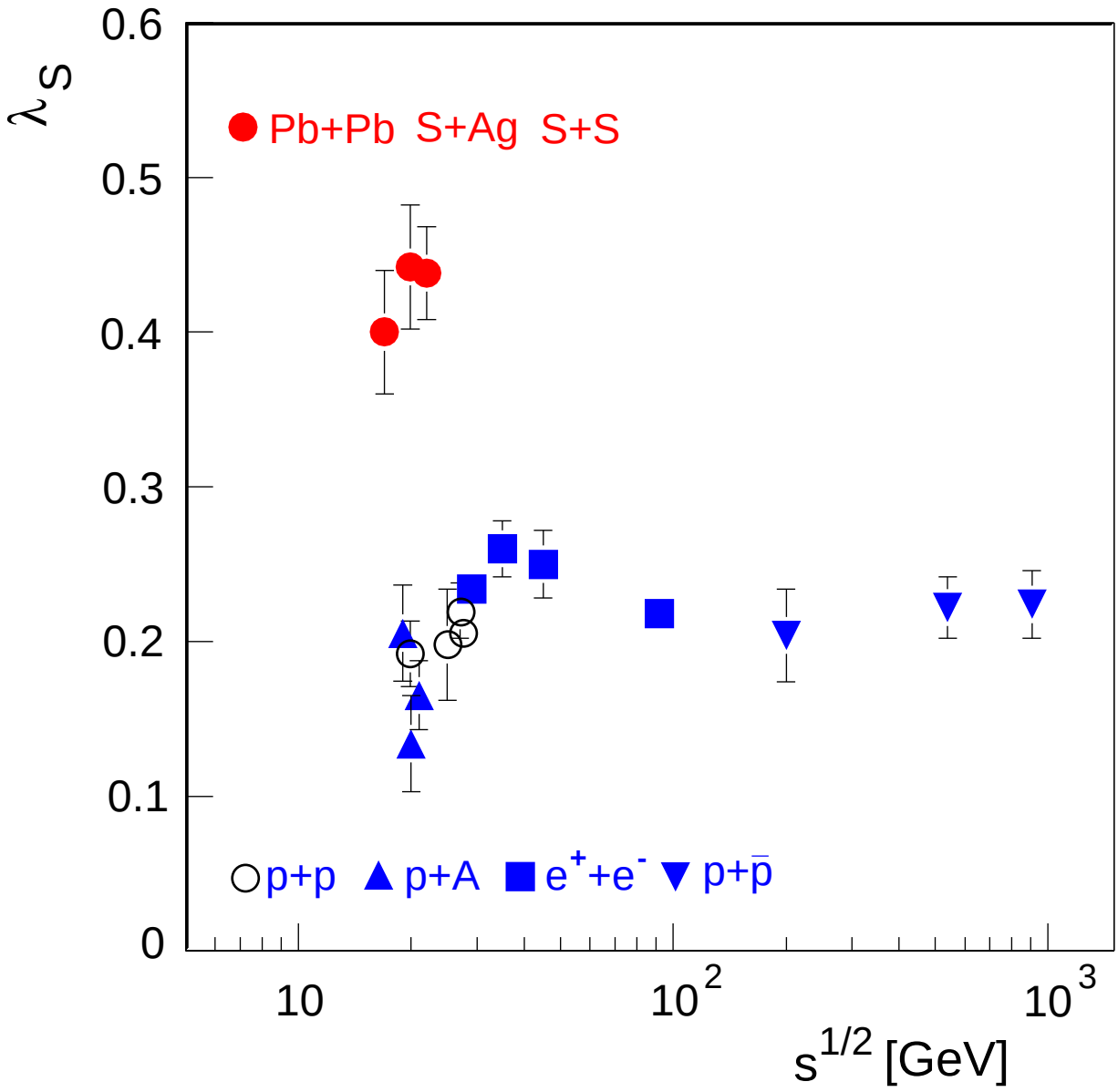


Figure 10: Strangeness suppression factor ($\lambda_S = \langle s + \overline{s} \rangle / (\langle u + \overline{u} \rangle + \langle d + \overline{d} \rangle)$ as a function of c.m. collision energy for different types of high energy interactions.

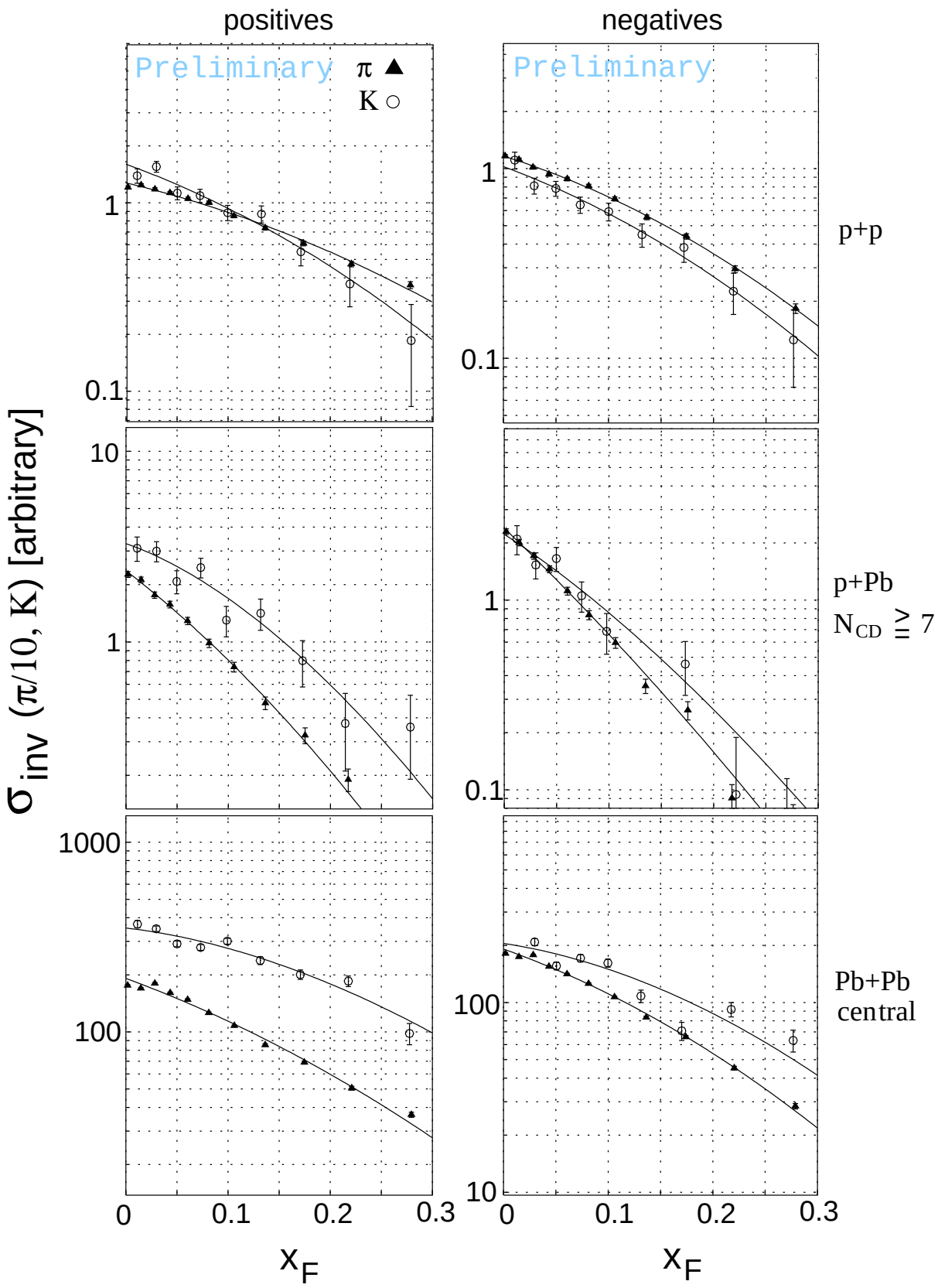


Figure 11: Invariant cross sections for charged pions and kaons as function of $x_F$ observed in p+p, central p+Pb, and central Pb+Pb collisions ($p_T$–range 400–500 MeV/c). The cross sections for pions are scaled down by a factor 10.

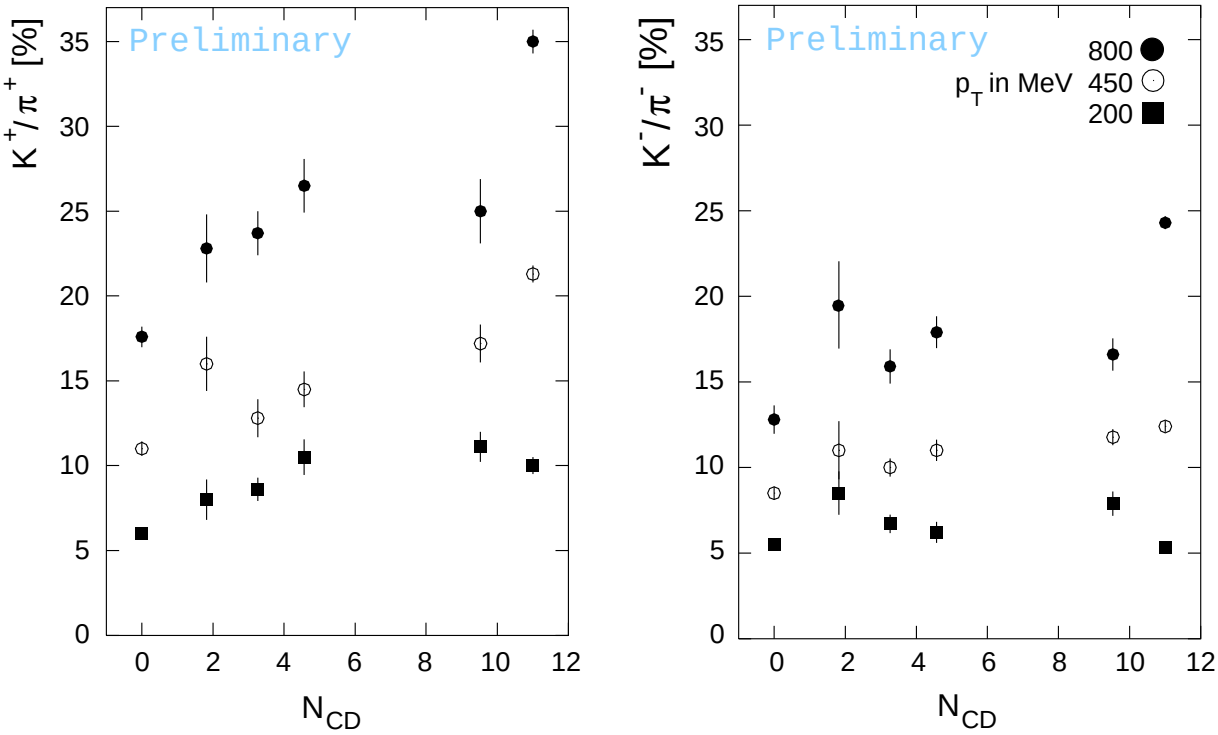


Figure 12: K/pi ratios at $x_F$=0.05 as function of p+Pb centrality ($N_{CD}$) for three $p_T$ ranges compared to p+p and central Pb+Pb collisions plotted at $N_{CD}$=0 and $N_{CD}$=11, respectively.

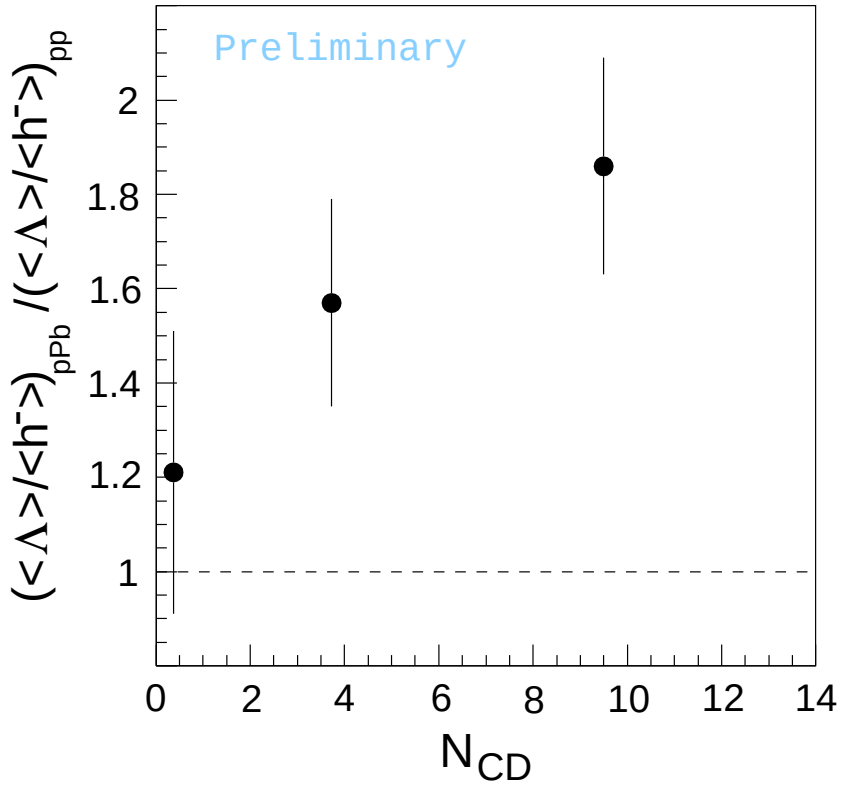


Figure 13: $\Lambda$/h$^-$ ratios for $\mid x_F \mid \leq 0.1$, referred to p+p, as function of p+Pb centrality.

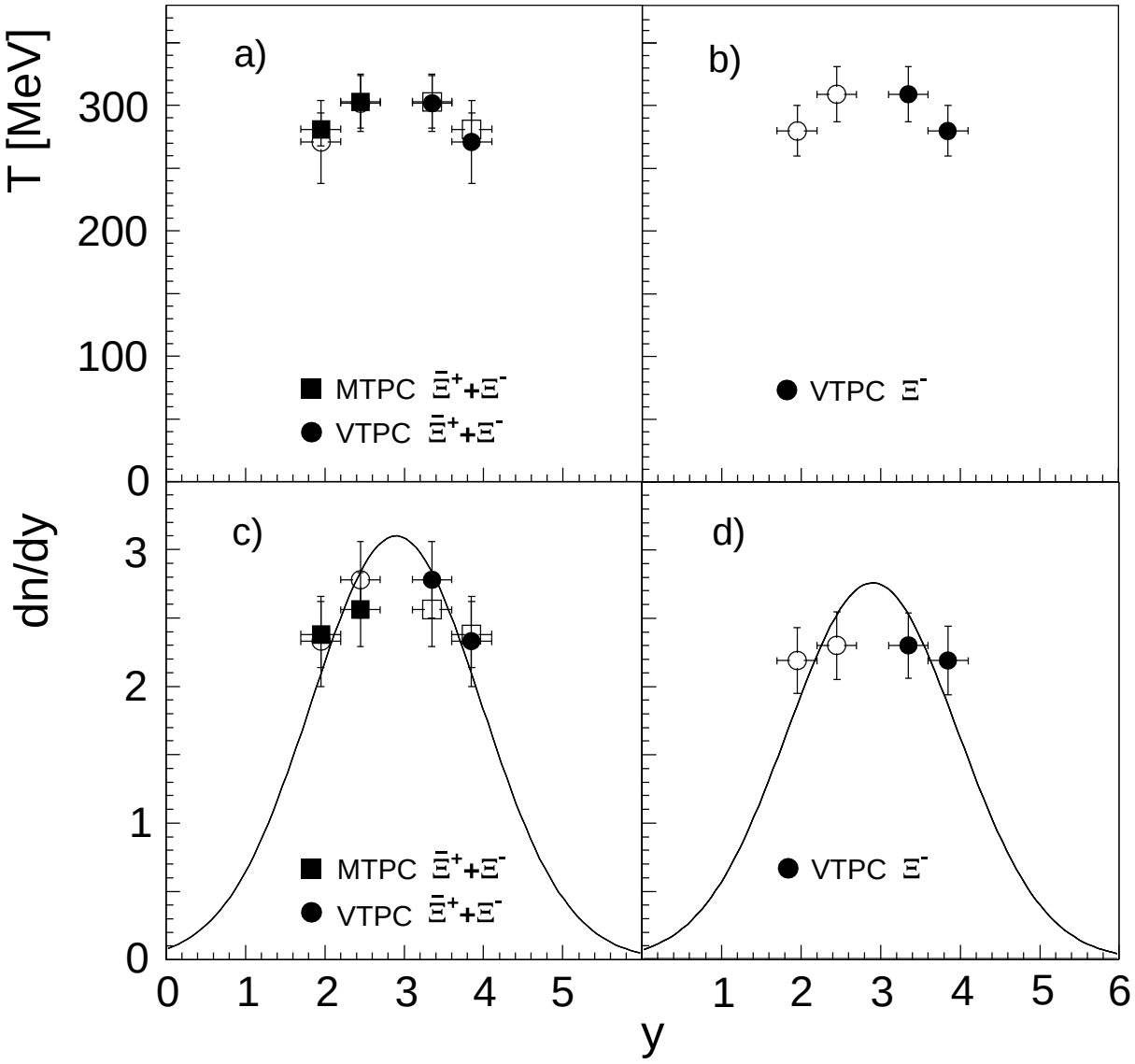


Figure 14: a), b) inverse slope of the transverse mass distributions and c), d) rapidity distributions of Ξ produced in central Pb+Pb collisions at 158 GeV/c per nucleon. (Open symbols are data points reflected around mid-rapidity.)

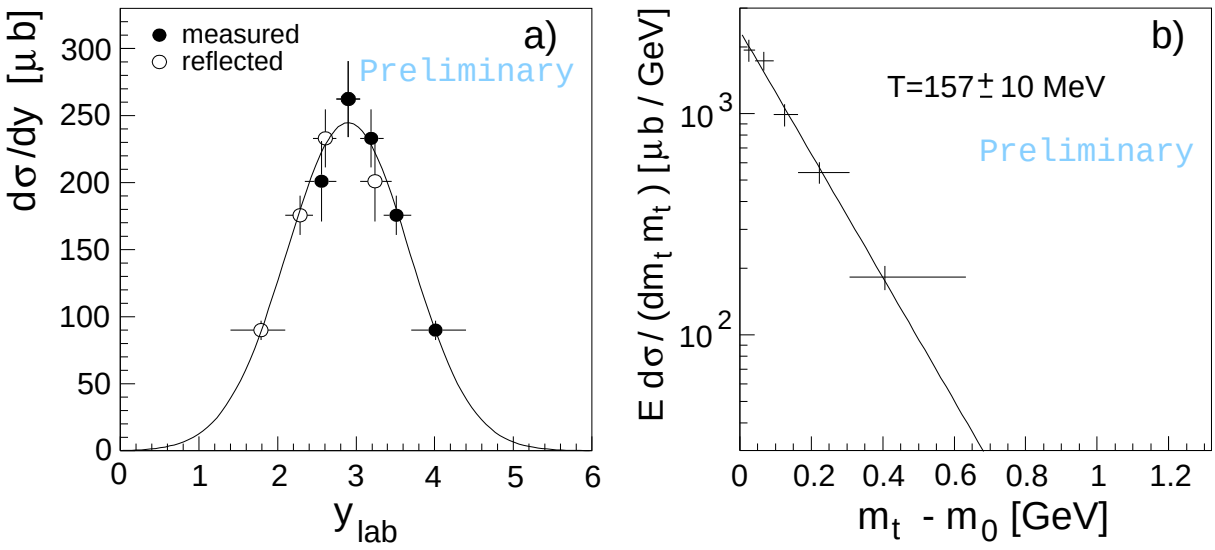


Figure 15: a) $y$ and b) $p_T$ distribution of $\Phi$ produced in p+p collisions.

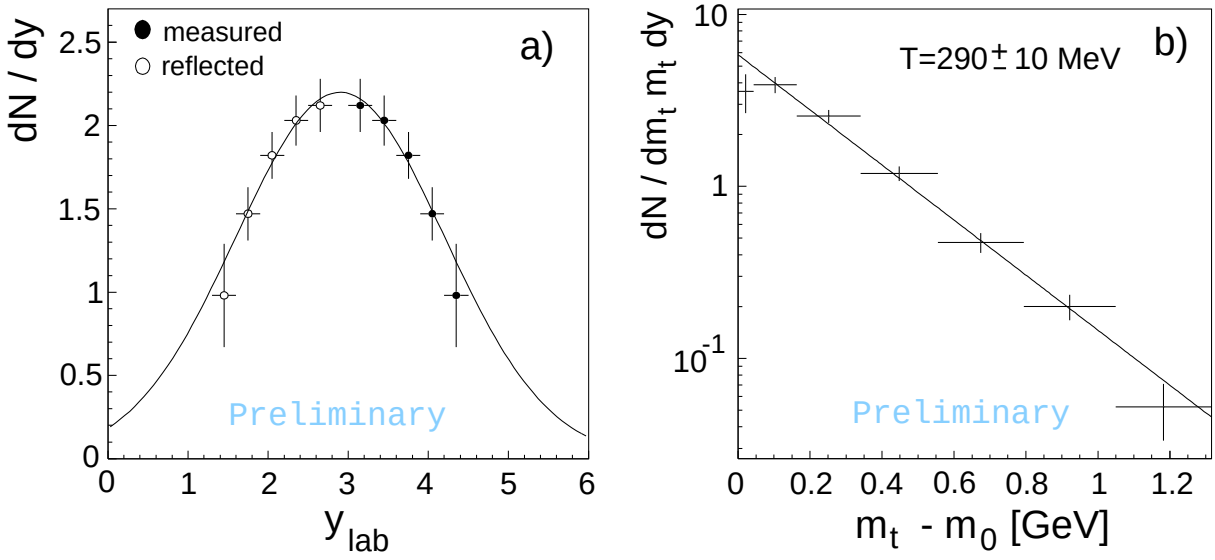


Figure 16: a) $y$ and b) $p_T$ distribution of $\Phi$ produced in central Pb+Pb interactions.

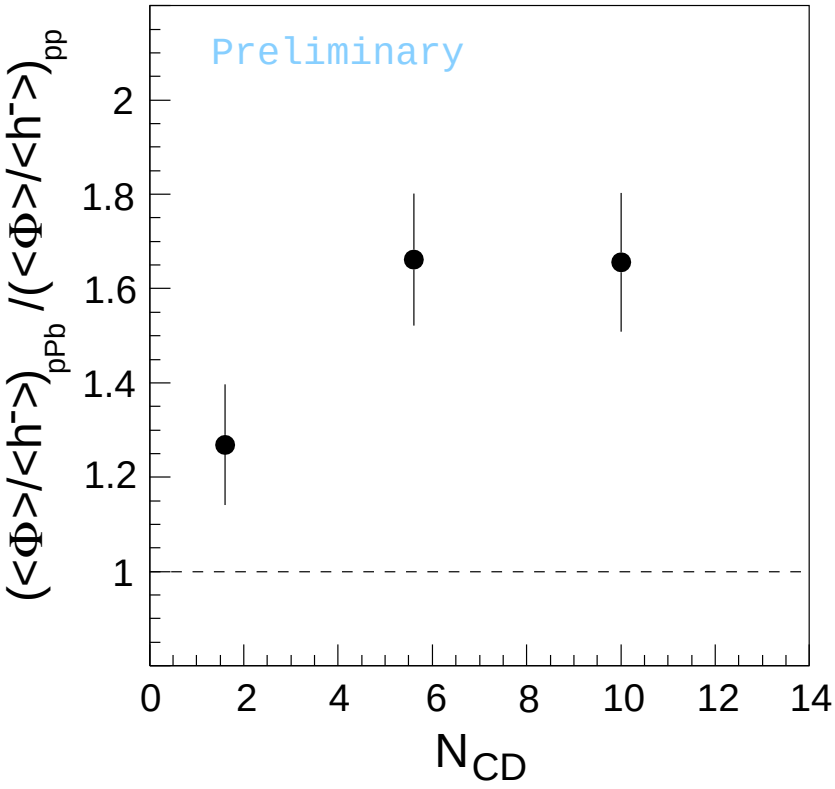


Figure 17: $\Phi/h^-$ ratios for $y \geq 2.5$, referred to p+p, as function of p+Pb centrality.

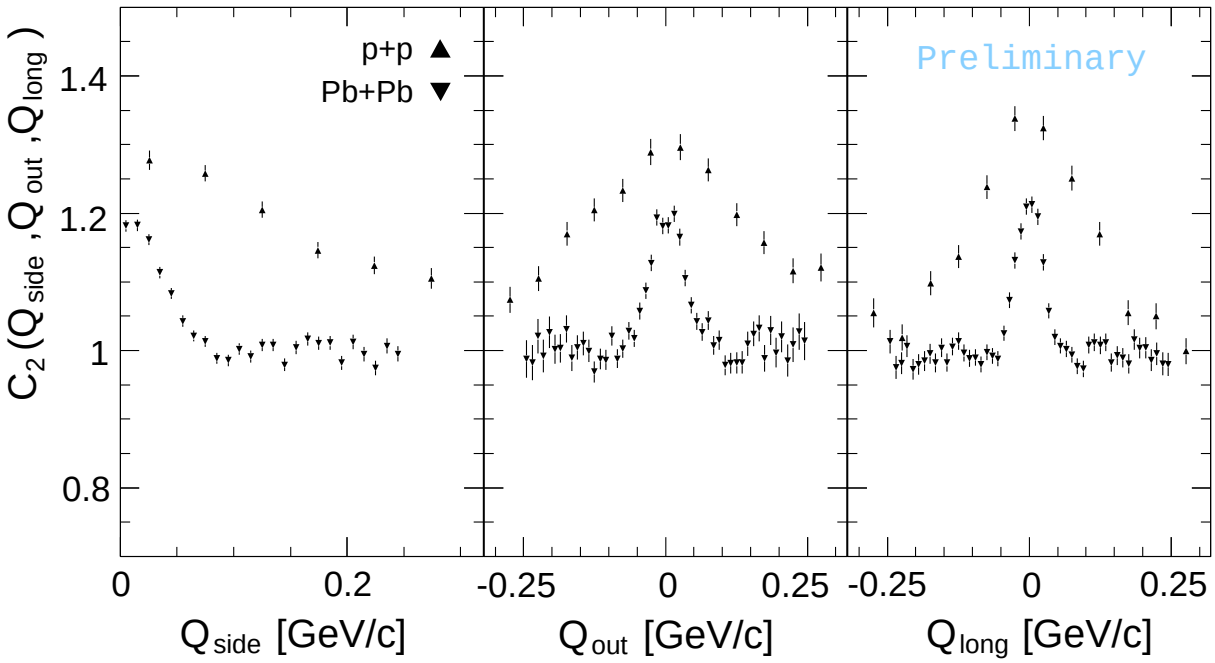


Figure 18: Comparison of correlation functions in the Bertsch–Pratt parametrization at mid-rapidity in p+p and Pb+Pb collisions.

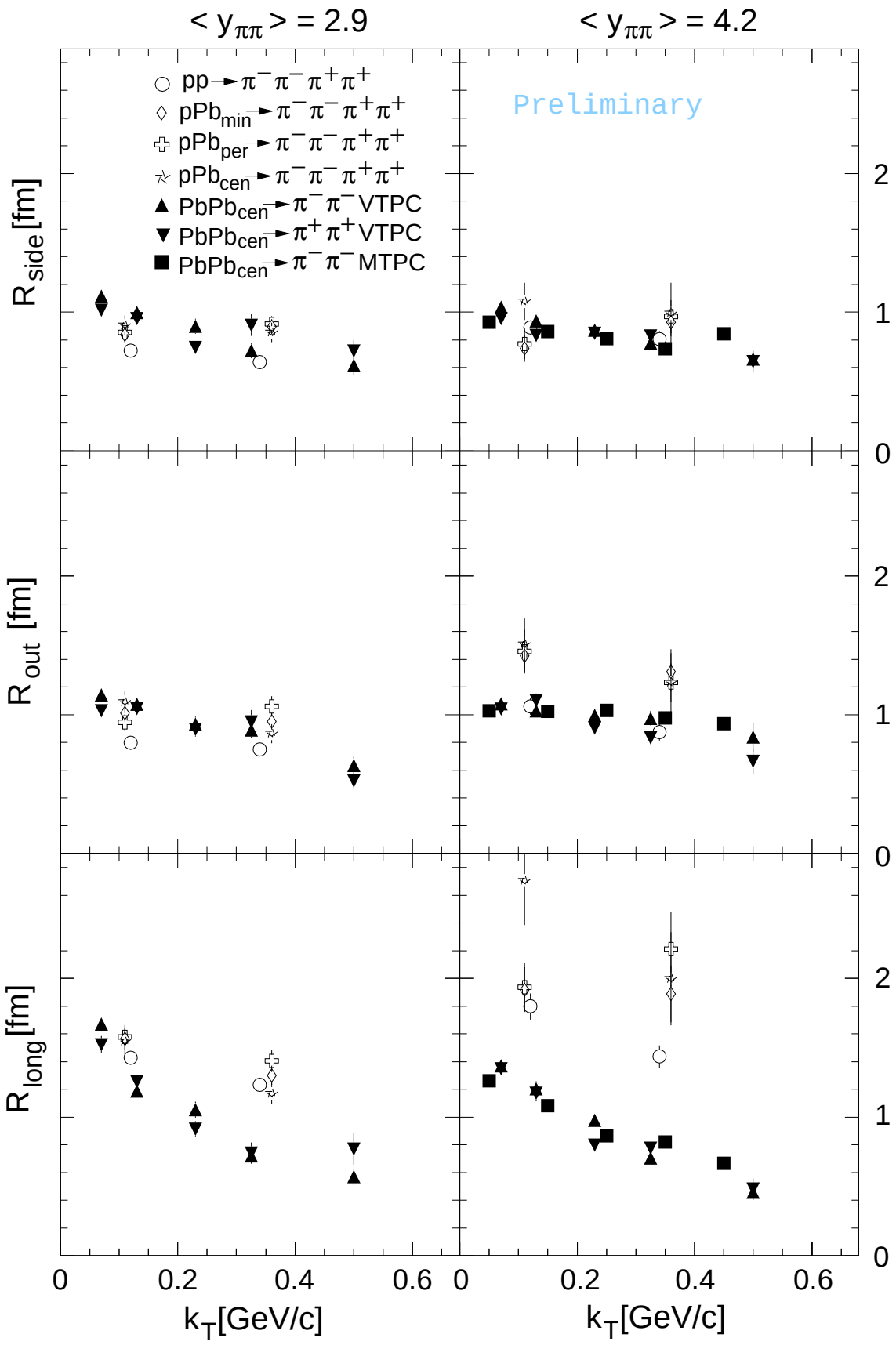


Figure 19: Radius parameters as function of $k_T$ obtained from 3-dimensional fits to the correlation functions with the Bertsch-Pratt parametrization for p+p, p+Pb, and Pb+Pb collisions. (Pb+Pb results have been scaled down by the geometry factor $A^{-1/3} = 1/6$.)

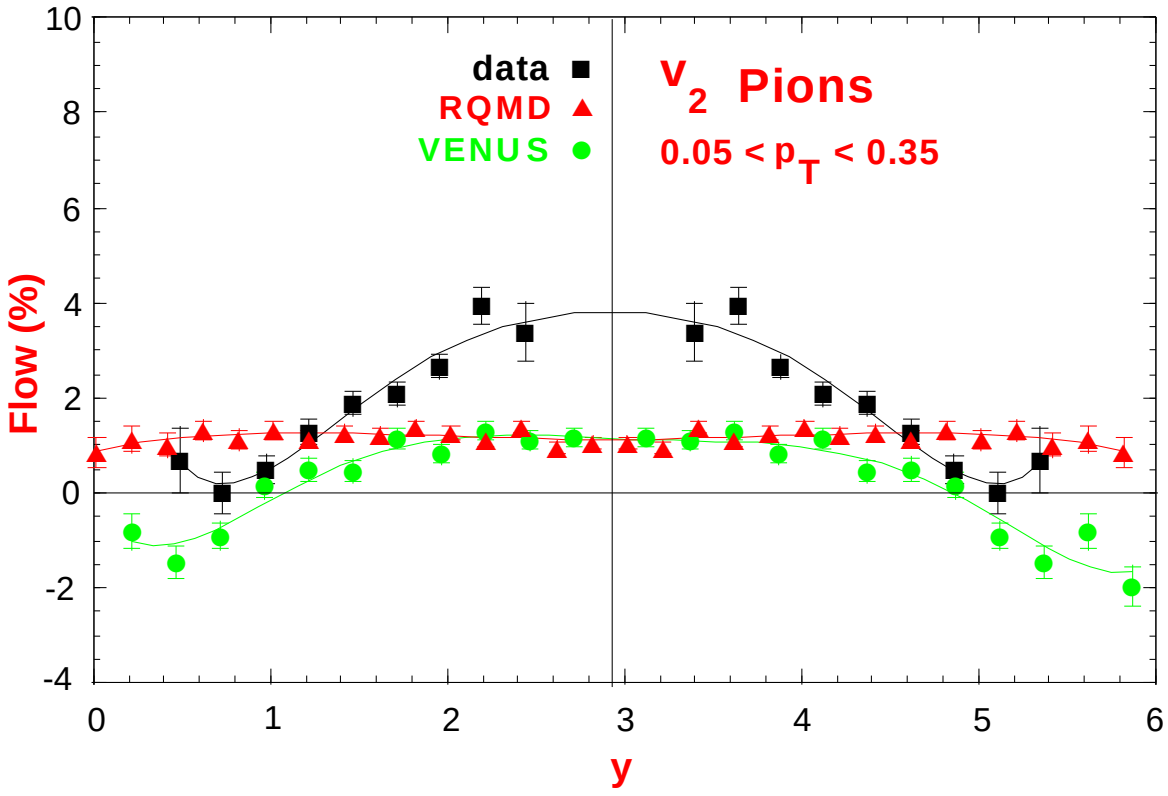


Figure 20: Rapidity dependence of elliptic flow for pions produced in medium impact parameter Pb+Pb collisions at 158 GeV/c per nucleon compared to the predictions of string–hadronic models [15]. (Data points below mid-rapidity are obtained by reflection.)